

Determination of pH by microfluorometry: intracellular and interstitial pH regulation in developing early-stage fish embryos (*Danio rerio*)

Andreas Mölich* and Norbert Heisler

Department of Animal Physiology, Humboldt-Universität zu Berlin, D-10115, Germany

*Author for correspondence (e-mail: andreas.moelich@rz.hu-berlin.de)

Accepted 9 September 2005

Summary

Microfluorometric techniques were applied *in vivo* for continuous monitoring of specific acid–base parameters in zebrafish (*Danio rerio*) embryos during early stages of ontogeny. Dextran-coupled pH-sensitive single-excitation/dual-emission dye SNARF-1 was pressure-injected into individual cells or the interstitial space of 16- to 256-cell embryos, and pH was continuously recorded during subsequent development for time periods of up to 8 h. A novel calibration technique was developed, essentially characterized by *in vitro* inorganic buffer calibration of the optical system and mathematical post-processing according to the effects of *in vivo* dye modifiers through a correlation established by direct comparison of optical techniques with pH microelectrodes. This approach results in high accuracy of microfluorometry, comparable with that of pH electrodes, and a recovery only limited by the physical stability of the utilized optical system.

Intracellular pH (pH_i) in *Danio rerio* embryos between 1k-cells stage and the end of epiboly was found to be well regulated to a mean value of 7.55 ± 0.13 (\pm S.D.), a range distinctly more alkaline than typical values for adult fish but in accordance with embryonic pH_i of a few non-fish species shortly after fertilization. Also, interstitial pH (pH_{int}) was significantly higher (8.08 ± 0.25) than values for

extracellular pH in adult fish. Distributions of HCO_3^- across membranes and between interstitium and ambient fluid compared with respective potentials strongly suggest that pH in these early stages of ontogeny is already adjusted by active transfer processes. Non-respiratory changes in ambient pH between 7.7 and 8.5 did not significantly affect pH_i , a result potentially attributable to low membrane leakage rate or to the potency of active transfer mechanisms. In order to assess the pH regulatory systems more quantitatively, embryos were exposed to ambient changes of carbon dioxide partial pressure (P_{CO_2}). The direct impact of P_{CO_2} changes on cell pH was alleviated by cell non-bicarbonate buffering and subsequent rapid, almost complete, compensation by changes in cell $[\text{HCO}_3^-]$ as an expression of transmembrane transfer of acid–base relevant ions. On the basis of these results, we conclude that the regulatory potency of embryonic cells is well developed, is active to resist extensive homeostatic stress and is efficient to maintain critical metabolism in adverse conditions, even at early stages of ontogeny.

Key words: intracellular pH, interstitial pH, ontogeny, regulation, transmembrane transfer, microfluorometry, *in vitro* calibration, intracellular microelectrode, *Danio rerio*, zebrafish.

Introduction

Regulation of pH, particularly of intracellular fluid compartments, is one of the main tasks of homeostatic regulation. Numerous vital processes critically demand energy supplied by metabolism. Metabolic flux, and thus energy production, is determined and often limited by the activity of key enzymes, e.g. phosphofructokinase (PFK), largely modulated by intracellular pH (pH_i). The limiting role of pH regulation becomes particularly evident during anaerobic muscular activity, when an extensive lactic acid-induced decrease of pH_i completely inhibits further contraction by reducing PFK activity to close to zero (cf. Heisler, 1982). Even more than in fully developed organisms, a high energy demand is expected in quickly growing and developing tissues, such as in embryos. Thus, adjustment of pH is a mechanism of homeostasis that is likely developed and activated quite early during ontogeny.

In fish and amphibians, much more than in mammals, birds and reptiles, embryos are exposed to challenges of pH regulation by direct contact with the aqueous ambient medium. With all changes in environmental composition, pH in the cells has to be maintained at values compatible with enzymatic function throughout development from single cells to multicompartmental animals. Not only the natural variability of the environment but also more recent and more severe impacts of coal mining and industry emissions provide considerable stress for developing organisms (e.g. Duis and Oberemm, 2000; Ingersoll et al., 1990). Numerous studies have focused on survival of fish eggs and fry in moderately and severely acidified waters (e.g. Johansson et al., 1973, 1977; Lacroix and Townsend, 1987). Mortality rises steeply at a water pH below 5, but loss of equilibrium and subsequent death is generally attributed to a net loss of ions from the body fluids,

particularly at low water $[Ca^{2+}]$ (Potts and McWilliams, 1989; Wood et al., 1990a), rather than to changes in body fluid pH.

The projected pattern of extensive ion loss as a cause of mortality may ultimately be related to lack of energy to drive ion transfer mechanisms, due to the inability to cope with the challenge for pH_i regulation (see above). In adult fish, extensive studies regarding acid–base regulation have been performed on a number of species and aspects (Claiborne, 1998; Heisler, 1986b, 1993), but, except for confusing results from a few studies at fertilization (Epel, 1997), hardly anything is known as to the regulatory facilities and capacities of cellular pH regulation during early development (1k-cells stage and above).

The present study has been designed to shed some light on pH regulation in intracellular and interstitial spaces during the early stages of ontogeny. Early stages of fish embryos provide some unusual and complicating features as compared with adult fish. The interstitial space is difficult to access for sampling, and acid–base-relevant ion exchange between body compartments, a common mechanism in adult fish (cf. Heisler, 1984, 1986b), is hampered during early ontogeny according to the delayed development of a defined extracellular space and the absence of circulation. Due to the lack of specialized structures, gas exchange is completely passive by diffusion through the external surface, and ion transfer between organism and environment is locally reduced to the external membranes of outer cell layers, rather than being performed by epithelial organs. With continuing ontogeny, the general regulatory capacity of the organism is expected to rise due to the development of gills, kidneys and other specialized structures.

This study was performed in embryos of zebrafish (*Danio rerio*), serving as an experimental model for pH regulation of developing fish. This species was chosen because of its wide use in ontogenetic research, with a well-founded background on care, breeding, preparation and development, as well as for its speed of embryonic development (3.7 days at 25°C; cf. Kimmel et al., 1995; Westerfield, 1995). Because of the requirement for non-destructive and quasi-continuous measurement over a relatively long time, pH was determined by application of laser-scanning-microfluorometry with specific dextran-coupled fluorescent dyes injected into studied fluid compartments before experimentation. After adaptation of this method to the very particular requirements of multicellular objects kept in an environment allowing normal ontogeny, the embryos were challenged by various external pHs, induced by either metabolic or respiratory means, in order to study characteristics of cellular and interstitial pH (pH_{int}) regulation.

Materials and methods

Animals

Adult zebrafish *Danio rerio* Hamilton 1822 of both sexes were obtained from a local supplier and kept in groups of 15–30 individuals in glass aquaria (35 litres), filled with

dechlorinated Berlin tap water. The aquarium water was recirculated through biological filters, aerated and maintained between 22 and 25°C. The animals were fed daily on commercial dry fish food *ad libitum* and kept at a fixed daily light regime of 11 h:1 h:11 h:1 h (light:transition:dark:transition).

Mating fish were separated in pairs in small tanks (~4 litres) during the light period. Fertilized eggs were collected the next morning after light-cycle dawn and transferred into embryonic medium (in mmol l⁻¹: NaCl 13.7, KCl 0.54, CaCl₂ 1.3, MgSO₄ 1, NaHCO₃ 5; modified from Westerfield, 1995). For experimentation, embryos were mechanically dechorionated. Adequate progress of embryonic development was checked by comparison with charts for standardized stages of development vs time after fertilization (recalculated for the experimental temperature of 25°C; Kimmel et al., 1995). (More detailed information on developmental stages of zebrafish, including pictures, is readily available at <http://zfin.org>; Sprague et al., 2001.)

Procedure

Intracellular and interstitial pH were measured, and further development of embryos was studied on the stage and in the light path of an inverse microscope assembly (Axiovert 135 M with attached LSM 410; Carl Zeiss, Jena, Germany). Water-soluble fluorescent dyes were pressure-injected through glass microcapillaries (tip diameter ~1 µm) into single cells of second or third layer or into the interstitium of embryos 2–3 h after fertilization (16-cell to 256-cell stages). Long-term compartment retention of dyes was promoted by using dextran-bound indicators, a measure also suitable to reduce compartmentalization, bleaching and cell damage by photolysis (Bright et al., 1989). These dyes proved to be stable for 8 h, until embryos underwent or finished epiboly.

Ambient conditions of the embryos were adjusted by continuous superfusion with embryonic medium adjusted in pH, ionic composition and respiratory gases. Embryos were kept in position over small funnel-like chamber exits by slight medium suction (Fig. 1), provided by a peristaltic pump. The resulting encircling flow for each individual proved suitable to provide well-defined media flow along the embryonic surface, preventing diffusion limitation on the basis of extensive unstirred layers. Unstirred layers and other elevations of resistance to diffusional gas exchange were found to cause unreproducible and largely drifting pH patterns, as observed in relevant preliminary experiments. In order not to affect the media composition by gas exchange with the ambient air, the air space of the chamber was flushed with the same gas as used for media equilibration.

After introduction into the experimental chamber, embryos were superfused with embryonic medium (containing 5 mmol l⁻¹ HCO₃⁻) for at least 2 h, in order to attain a steady state, before embryos were exposed at 2 h intervals to changing acid–base conditions by alternating superfusion with media of other characteristics. Media utilized for

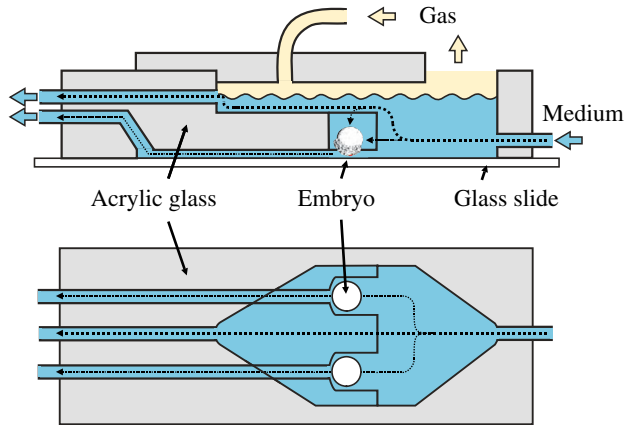


Fig. 1. Principle of experimental chamber utilized in all series of experimentation. Embryos were fixed over small funnel-like chamber exits by slight medium suction. Stratification on the basis of diffusion limitation is prevented by the encircling flow of medium, provided by a peristaltic pump. The air space of the chamber was flushed with the same gas as used for equilibration of the medium.

superfusion were conditioned by equilibration with gas mixtures of air and CO_2 , produced with precision gas-mixing pumps (Digamix 1M301 and 2M302; Wösthoff, Bochum, Germany) and humidified at the experimental temperature of 25°C. pH in fluid compartments of the embryos was challenged in separate experimental series by respiratory or metabolic (non-respiratory) changes of media pH. Respiratory changes were effected at a constant $[\text{HCO}_3^-]$ of 5 mmol l^{-1} by equilibration with different P_{CO_2} s of either 0.73, 2.4, 7.4 or 24.6 mmHg (0.1, 0.32, 1.0 or 3.3 kPa), resulting in media pH values of 8.43, 7.93, 7.44 or 6.92, respectively. Changes in media $[\text{HCO}_3^-]$ (2, 5, 20 mmol l^{-1}) at a constant P_{CO_2} of 2.4 mmHg (0.32 kPa) effected non-respiratory changes in ambient pH (pH_{amb} ; 7.54, 7.93, 8.48, respectively).

Adequate development of embryos under severe hypercapnia was studied in a separate series. Two groups of dechorionated embryos of similar stage were exposed in embryonic medium to P_{CO_2} s of 2.4 mmHg (0.32 kPa; $N=20$) and 24.6 mmHg (3.28 kPa; $N=20$). Ontogenetic progress was monitored and compared between the two groups as well as with non-dechorionated, completely unhandled embryos at normocapnia after 3 and 24 h of exposure.

Analytical approach

Microfluorometric determination of pH

Embryonic pH_i and pH_{int} were determined by single-excitation/dual-emission or dual-excitation/single-emission fluorometry using pH-sensitive dyes coupled to 10 kDa dextran molecules (Molecular Probes, Eugene, OR, USA). Dyes were excited by laser light of an appropriate wavelength, and the emission was monitored by high-sensitivity photomultipliers. Laser bands of excitation were selected, and emission channel ranges were discriminated by wavelength-selective beam

splitters, high-pass, low-pass and notch interference filters, where appropriate.

On the basis of published wavelength spectra, two fluorescent dyes were originally selected as suitable for the project: SNAFL-2 {Seminaphthofluorescein; 9-chloro-3,10-dihydroxy-spiro [7H-benzo(c)xanthene-7,1'(3'H)-isobenzofuran]-3'-one} and SNARF-1 {Seminaphthorodafuor; 10-dimethylamino-3-hydroxy-spiro[7H-benzo(c)xanthene-7,1'(3'H)-isobenzofuran]-3'-one}. Differentiation between ionized and non-ionized forms of the indicator was achieved for SNAFL-2 by dual-wavelength channel excitation by subsequent selective exposure to laser lines at 488 nm ('extended blue' argon) and 543 nm (helium–neon), respectively, selected by an AOTF (acousto-optical-transmission-filter) wavelength-selective shutter system for each 4 s. The resulting fluorescence was picked up in one common emission channel at wavelengths $>570 \text{ nm}$. Single-wavelength excitation of SNARF-1 by an extended blue argon laser at 488 nm results in fluorescent emission picked up simultaneously for the ionized dye form at wavelengths of 590–610 nm and that of the non-ionized form at $>630 \text{ nm}$. The ratio of fluorescent activities is accordingly a function of pH at the indicator site (for details, cf. Whitaker et al., 1991). Ratiometric determination carries the advantage of being independent of the absolute concentration of the dye as well as of variable optical density of apparatus light path and biological matrix.

Optical stability of instrumentation

Short- and long-term stabilities of the optical system (including lasers, light path components and detectors) were checked in a series of preliminary experiments. Solutions of 2–5 $\mu\text{mol l}^{-1}$ SNARF-1 or SNAFL-2 in 100 mmol l^{-1} phosphate buffer at constant pH (~ 7.2) were exposed to laser excitation in a temperature-controlled sample chamber, and the emissions were monitored as a function of time every 5 min for 4.5–5 h. Emission intensities were corrected for autofluorescence (essentially, photomultiplier offset and noise) and normalized to the initial value. In order to differentiate between instabilities brought about by variability of laser intensity and changes of fluorescent dye characteristics by bleaching or local aggregation of attached dextran, measurements were referenced to a fluorescent uranium glass standard (type F53; Carl Zeiss), with its fluorescent quantum efficiency being only affected according to the decay of radioactivity (half-life $\sim 4.5 \times 10^9$ years).

Choice of indicator type

With dual-excitation, single-emission dyes like SNAFL-2, the differential variability between two excitation sources (488 nm and 543 nm) is directly transmitted into the emission intensity ratio. Long-term instability can be corrected for by carrying along a fixed fluorescent reference (e.g. uranium glass; see above), but in this specific case the long-term instability was superposed by additional short-term variability (flutter) of excitation intensities. Due to direct transmission of excitation flutter into four non-simultaneous determinations of

fluorescent emission, the successive two-standard and two-sample excitations required for fixed standard referencing will, in the worst case, duplicate the maximal error rather than correcting short-term fluctuations.

Consequently, the present project was conducted utilizing the dual-emission dye SNARF-1. Simultaneous dual emission cancels instabilities of excitation sources and light path, but optical instabilities of the required two emission paths cannot be eliminated by any means. The magnitude of fluctuations in the emission path, however, was relatively small as compared with that originating in laser excitation.

The SNARF-1 fluorescence ratio (R) relating to absolute pH calibration (see below) calculates:

$$R = (F1_{\text{sam}} - AF1_{\text{sam}})/(F2_{\text{sam}} - AF2_{\text{sam}}), \quad (1)$$

where $F1_{\text{sam}}$ and $F2_{\text{sam}}$ are sample fluorescence intensities at wavelengths 1 or 2, respectively, and AF is autofluorescence.

Calibration of the optical system

In biological fluids, dyes are subject to modification of their physicochemical and optical characteristics due to the presence of proteins, nucleotides and other binding and interfering matter. Accordingly, *in situ* calibration is advantageous, as long as the prevailing pH is precisely known.

Ionophore calibration

In situ calibration procedures are based on equalizing intracellular with extracellular conditions by application of ionophores such as nigericin (e.g. Thomas et al., 1979), effecting a transmembrane K^+/H^+ exchange with relative selectivity (Pressman, 1976). However, in multicellular/multilayer preparations, the expected effect is usually not achieved, as indicated by preliminary experiments. In intact tissues and organisms, the procedure is probably hampered by long diffusion pathways and tightly interlaced cell layers, resulting in variable and unpredictable intracellular pH and ionic concentration values (N. Heisler and J. Wasser, unpublished; N. Heisler and N. Gonzalez, unpublished). As a further major obstacle, organisms are frequently destroyed by application of nigericin and the required extremely high extracellular $[K^+]$ (A. Mölich and N. Heisler, unpublished).

In vitro calibration

In order to avoid obstacles and limitations of *in situ* ionophore calibration, the effect of biological fluid components on physicochemical and optical characteristics of SNARF-1 was mimicked *in vitro*. The optical system was calibrated with SNARF-1 standards, modified by addition of either 100 mmol l^{-1} inorganic phosphate, 2.5, 5 or 10% bovine serum albumin (BSA; Fraction V; Sigma-Aldrich, Deisenhofen, Germany) and/or 150 mmol l^{-1} KCl. pH-adjusted, modified standards were used for *in vitro* calibration of the optical system before determination of pH in embryonic cells and interstitium. The quality of simulation was simultaneously determined in the same cell or the interstitium by microelectrodes as an independent reference (see below).

Although the behaviour of SNARF-1 in biological fluid compartments could well be approximated by an aqueous *in vitro* mixture of cellular components, mock fluids could not be used for calibration because of a pronounced instability of the protein-containing solutions. Accordingly, the optical technique was calibrated *in vitro* with 100 mmol l^{-1} phosphate buffers. The *in vivo*-induced property shifts of SNARF-1 were corrected for by mathematical post-processing, based on the relationship established from *in vivo* comparison of the *in vitro* phosphate-buffer-calibrated optical system with simultaneous pH-sensitive intracellular or interstitial microelectrode measurements at the same site.

pH-sensitive microelectrodes

pH-sensitive liquid ion exchanger microelectrodes (LIX) were built with slight modification of methods described by Voipio et al. (1994). In brief, double-barrelled monofilament borosilicate glass tubing (type 2GC150FS7.5; Clark Electromedical Instruments, Pangbourne, UK) was pulled to tip diameters of $\sim 1 \mu\text{m}$. After silanizing one barrel by exposing the tip to vapor of *n,n*-dimethyltrimethylsilylamin (Fluka, NeuUlm, Germany), the electrode was dry-bevelled to a point (tip diameter 2–5 μm) at an angle of about 45° . The silanized barrel was backfilled with buffer solution (NaCl 100 mmol l^{-1} , Hepes 50, NaOH 25, pH 7.8), and the tip filled with H^+ -ionophore (Hydrogen Ionophore I-Cocktail B; Fluka) by gentle suction. The unsilanized barrel was filled with 150 mmol l^{-1} KCl, serving as a reference for the pH electrode. The two barrels were each connected to high-impedance voltage followers ($10^{15} \Omega$; AD515A operational amplifiers; Analog Devices, Norwood, MA, USA) by chlorinated silver wires. The potentials of both electrode channels, referenced to an extra-embryonic double agar-bridge Ag/AgCl electrode, were amplified independently using high-stability laboratory isolation amplifiers (custom-made; N. Heisler and H. Slama, unpublished) and were recorded by computer-aided data acquisition (A/D-converter, DAS 1602; Keithley, Taunton, MA, USA; software, Test Point 3.3; Capital Equipment Corp., Billerica, MA, USA). The pH signal as the difference of the two channels was calibrated with 100 mmol l^{-1} phosphate buffers.

Analysis of optical data

Fluorescence intensities were scanned in matrices of 128×128 locations, with each location digitized with a resolution of 8 bit. The biological projection area represented by each scan field is approximately $450 \times 450 \text{ nm}$ with the generally used 20×0.40 Zeiss LD-Achroplan lens. The obtained matrices of fluorescence intensities were stored as raster images in tag-based image file format (TIFF; 8 bit intensity). The overall sensitivity of the analog detection system was carefully adjusted by photomultiplier analog gain and anodes high voltage to allow dynamic pH changes without clipping intensities by exceeding the range of digitization (8 bit). According to the general range adjusted during experimentation ($\sim 1 \text{ pH unit}/8 \text{ bit}$) the theoretical resolution of the apparatus is $\sim 0.004 \text{ pH units}$.

Intensity ratios were calculated for each individual scan field (Eqn 1). Since dividing two groups of normally distributed data by each other results in a logarithmic distribution, all subsequent averages were calculated from log-transformed data. Average ratios accordingly represent true average pH of the area utilized for calculation. The obtained raw average pH data were referenced to the calibration data obtained by fluorescent measurement of SNARF-1 in 100 mmol l⁻¹ phosphate buffer of specified pH and were corrected according to mathematical post-processing (pp) for the correlation between optical phosphate buffer calibration and microelectrode response (Eqns 2, 3; see also above) for the intracellular space ($r^2=0.978$, $N=213$):

$$\text{pH}_{\text{pp}} = 1.0556 \text{ pH}_{\text{raw}} - 0.1821, \quad (2)$$

and for the interstitial space ($r^2=0.879$, $N=111$):

$$\text{pH}_{\text{pp}} = 1.3575 \text{ pH}_{\text{raw}} - 2.4048. \quad (3)$$

These relationships are independent of the optical equipment used and may be applied to similar biological approaches.

Calculations

Calculations based on the Henderson–Hasselbalch equation were conducted using constants derived from the relationships of Heisler (1984, 1986a, 1989), applying the experimental temperature of 25°C and parameters for typical fish cell fluid (molarity, 0.281 mol l⁻¹; ionic strength, 0.220; [Na⁺]=0.012 mol l⁻¹; [protein]=200 g l⁻¹) and interstitial composition (molarity, 0.270 mol l⁻¹; ionic strength=0.140; [Na⁺]=0.130 mol l⁻¹; [protein]=0 g l⁻¹). Bicarbonate concentrations were calculated from measured pH and applied P_{CO_2} . According to short diffusion distances and high CO₂ diffusivity, intraembryonic P_{CO_2} was assumed to be equal to ambient values. Apparent nonbicarbonate buffer values ($\beta_{\text{NB,app}}$) were calculated as ratios of deflections of pH and [HCO₃⁻] (Heisler, 1986a). Maximal deflections of measured pH after about 10 min indicated that equilibration to the new P_{CO_2} was safely complete after this time period.

The equilibrium potentials for the distribution of bicarbonate between intracellular and interstitial spaces as well as between interstitial and ambient fluids were calculated on the basis of compartmental concentrations by application of the Nernstian equation.

Results

Validation of optical techniques for pH determination

Accuracy as well as recovery of pH data determined by the applied optical techniques critically depends on the stability of the instrumentation used. Surprisingly, and in contrast to the specifications of the applied apparatus, the obtained fluorescent emissions from a variety of dye standards were extremely variable. Analysis at different points of the overall light path attributed the observed variability of fluorescence mainly to instability of laser intensity, but inconstant light transmission in AOTF and other optical components also contributed

significantly. Fluctuations of more than 50% within 5 h were noted for each of the two used lasers (extended blue argon laser, 488 nm, and helium–neon laser, 543 nm; Fig. 2). Unfortunately, emission intensities varied independently for excitation with the two lasers, such that, in worst case conditions, negative shifts of one laser would be accompanied by positive shifts of the other to add up to 70 or 80% change in fluorescence ratio with dual excitation (SNAFL-2) (cf. Fig. 2). Lasers did not become stable even after ‘warm up’ periods of many hours (8–16 h). The variability was found to be affected by accurate beam adjustment at various optical components, but repeated readjustment by manufacturer service personnel according to the book did not result in a stability better than the original values.

Partial compensation of this most disturbing phenomenon was possible by carrying along a uranium-glass standard, which reduced long-term drift of the detection ratio. Short-term

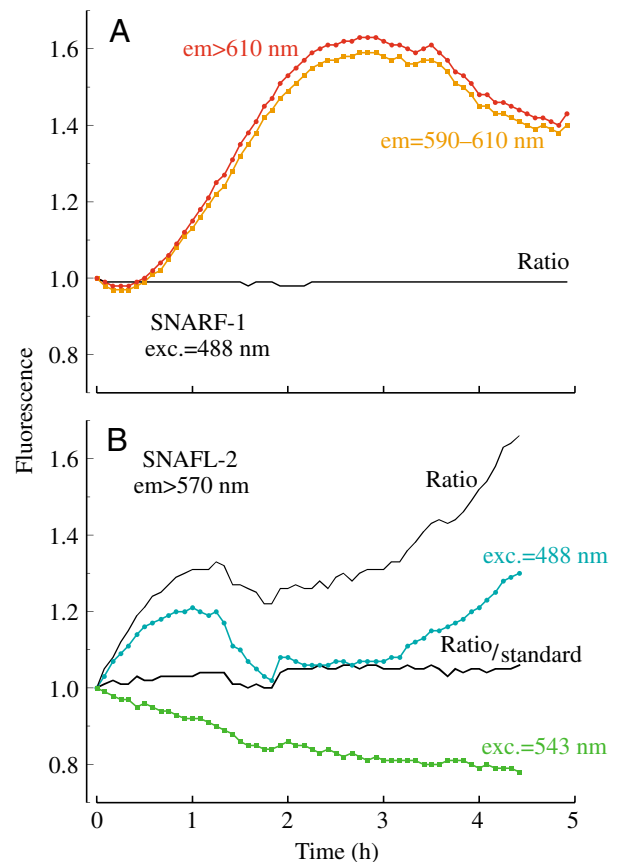
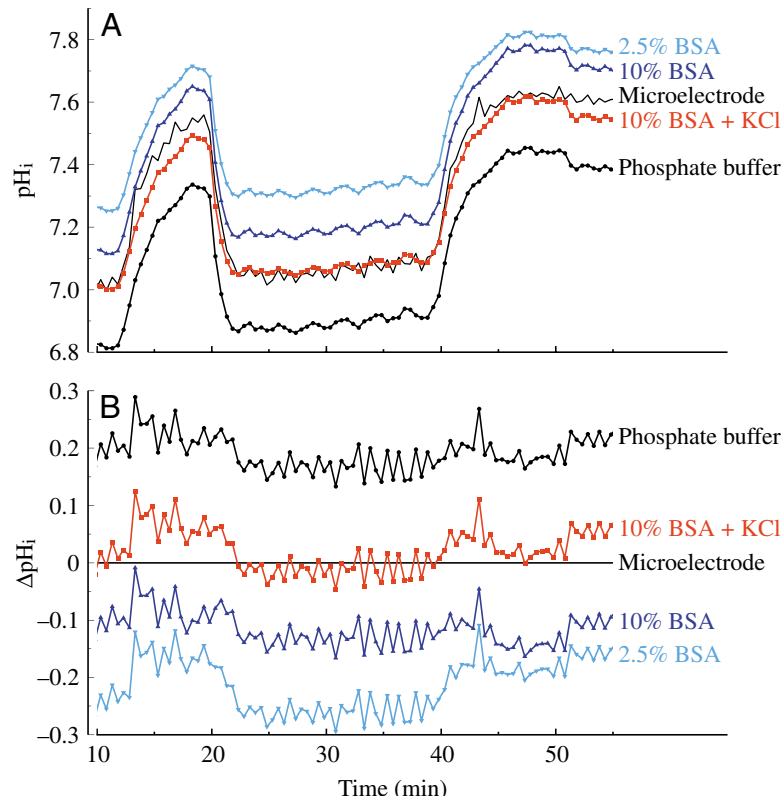


Fig. 2. Fluorescence intensities and intensity ratios of aqueous phosphate-buffered standards upon excitation of SNARF-1 (A) at 488 nm (dual-emission detection at 590–610 nm and >630 nm) and of SNAFL-2 (B) at 488 nm and 543 nm (emission detection at >570 nm). The extensive long-term laser instability is compensated for by ratiometric analysis ($\pm 2\%$) with the dual emission dye SNARF-1 (A), but is additionally transmitted into the intensity ratio of the dual excitation dye SNAFL-2 (B). Referencing SNAFL-2 signals to quasi-simultaneous measurements of a fluorescent uranium glass standard is suitable to reduce fluctuations to $\pm 6\%$. Abbreviations: exc., excitation wavelength; em, emission wavelength.

variability could not be compensated and resulted in a variability of the fixed standard-corrected ratio of $\pm 6\%$ (Fig. 2B). This amount of noise is still three times as large as for measurement of SNARF-1 ($\pm 2\%$; single excitation, 488 nm) with dual-emission detection at 570–590 nm and >630 nm, without uranium glass standard (Fig. 2A).

Calibration of optical measurements

Comparative determination of pH_i by optical SNARF-1 measurements and pH-sensitive intracellular microelectrodes indicated distinct differences. Calibrating the optical analysis *in vitro* with phosphate buffers revealed a difference of the determined pH to the acidic side by ~ 0.2 units, while calibration with protein-containing media shifted the resulting pH by 0.1–0.3 units to the alkaline side as compared with microelectrodes (Fig. 3). The best concordance between the two analytical approaches was achieved with a combination of 10% BSA and 150 mmol l^{-1} KCl, resulting in an average absolute deviation of less than 0.07 pH units compared with microelectrodes and a 95% confidence interval of 0.04 pH units for the fit of pH vs SNARF-1 fluorescence ratio. Since physicochemical instability of this best simulation of intracellular conditions did not allow direct use for calibration, the optical system was directly referenced to simultaneous microelectrode readings. The absolute accuracy obtained from *in vitro* calibration with pure phosphate buffers and mathematical correction for intracellular factors is accordingly limited only by system-immanent deviations of secondary electrodes as compared with the hydrogen electrode standard.



Acid–base parameters of embryonic zebrafish

Intracellular and interstitial pH in the studied early stages of embryonic development during control conditions were maintained relatively constant at 7.55 ± 0.13 and 8.08 ± 0.25 , respectively ($\bar{x} \pm \text{s.d.}$). Non-respiratory changes of ambient pH induced by varying ambient bicarbonate concentration did not affect cell pH, at least not in the tested, slightly alkaline range of 7.5 to 8.5. By contrast, changes in ambient P_{CO_2} were transmitted immediately to the embryonic fluid compartments, effecting rapid changes in pH_i and pH_{int} (Figs 4, 5: different levels of hypercapnia; Figs 6, 7: post hypercapnia). Upon exposure to a new P_{CO_2} , maximal deflection of pH_i and pH_{int} was attained after ~ 10 min. In spite of the extensive (10-fold) change in P_{CO_2} , the maximal average pH deflection was limited to ~ 0.25 – 0.65 units in intracellular and 0.35 – 0.9 units in interstitial fluid compartments, equivalent to apparent $\beta_{\text{NB,app}}$ values of 10 – $25 \text{ meq. pH}^{-1} \text{ l}^{-1}$ and 0 – $85 \text{ meq. pH}^{-1} \text{ l}^{-1}$, respectively. In the following two hours, pH was returned towards the original value, with the majority of the theoretical shift compensated by changes in compartmental $[\text{HCO}_3^-]$ (75–96%; cf. Heisler, 1986c) (Figs 4–7). $[\text{HCO}_3^-]$ changed between 5.6- and 9-fold in intracellular compartments and between 2.5- and 8.9-fold in the interstitial space. The compensation process started to level off but was not complete after 2 h of exposure to the new P_{CO_2} . At this time, $\beta_{\text{NB,app}}$ values were attained between 37 and $170 \text{ meq. pH}^{-1} \text{ l}^{-1}$ for intracellular space and between 44 and infinity for the interstitium.

The Nernstian equilibrium potentials for the distribution of bicarbonate between intracellular and interstitial space, as well as between interstitial space and ambient fluid, changed considerably in response to changes in P_{CO_2} and the resulting changes in bicarbonate concentrations (Figs 4–7, lower panels).

Development of zebrafish embryos in hypercapnic environments

Comparison of two groups of zebrafish developing under moderately ($P_{\text{CO}_2} = 2.4 \text{ mmHg}$, 0.32 kPa) and severely ($P_{\text{CO}_2} = 24.6 \text{ mmHg}$, 3.3 kPa) hypercapnic conditions with control, unmanipulated animals at normocapnia revealed no significant differences in ontogenetic development during the observation period of 24 h, in spite of largely different environmental pH (7.93 and 6.92 for P_{CO_2} of 2.4 and 24.6 mmHg, respectively). The observed mortality of

Fig. 3. Determination of intracellular pH (pH_i) with intracellular microelectrodes and by application of microfluorometry of SNARF-1-dextran, calibrated with standards containing 100 mmol l^{-1} phosphate, BSA and 150 mmol l^{-1} KCl. Embryonic cells were equilibrated with P_{CO_2} s alternating between 2.4 and 24.6 mmHg (A). Differences of optical measurements as compared with microelectrode readings indicate the best approximation to intracellular conditions to be achieved by addition of 10% BSA + 150 mmol l^{-1} KCl (B).

~50% during the 24 h monitoring period was higher than during normal undisturbed growth but was the same in both observation groups. Reduced survival in this experimental series has to be attributed to extensive and repeated handling and agitation in the aeration chamber of sensitive and fragile embryos deprived of their natural protective cover by dechorionation. Although transition of the surviving embryos to specific stages was slightly delayed (~15%) compared with standard charts (corrected for 25°C; Kimmel et al., 1995), the

pattern of developmental transitions was identical to control groups of animals undisturbed by any experimental manipulation. Also, deviations from the standard morphology of embryos were not found at any time.

Discussion

Optical measurement of intracellular and interstitial pH
Determination of pH with optical, non-destructive methods

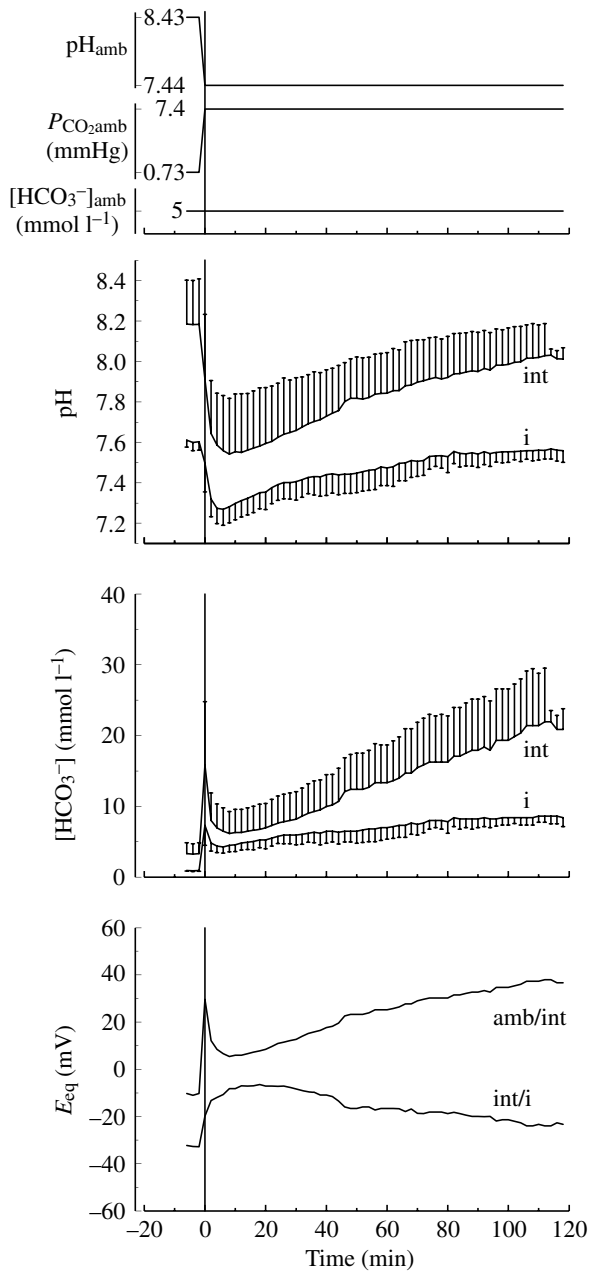


Fig. 4. Hypercapnia in *Danio rerio*. pH, $[HCO_3^-]$ and HCO_3^- equilibrium potentials (E_{eq} ; according to the Nernst equation) of fluid compartments of *Danio* embryos in response to 10-fold changes in P_{CO_2} from 0.73 to 7.4 mmHg. Indices denote: amb, ambient; int, interstitial; i, intracellular. Each point represents the mean of 7 (i) or 6 (int) measurements \pm S.D.

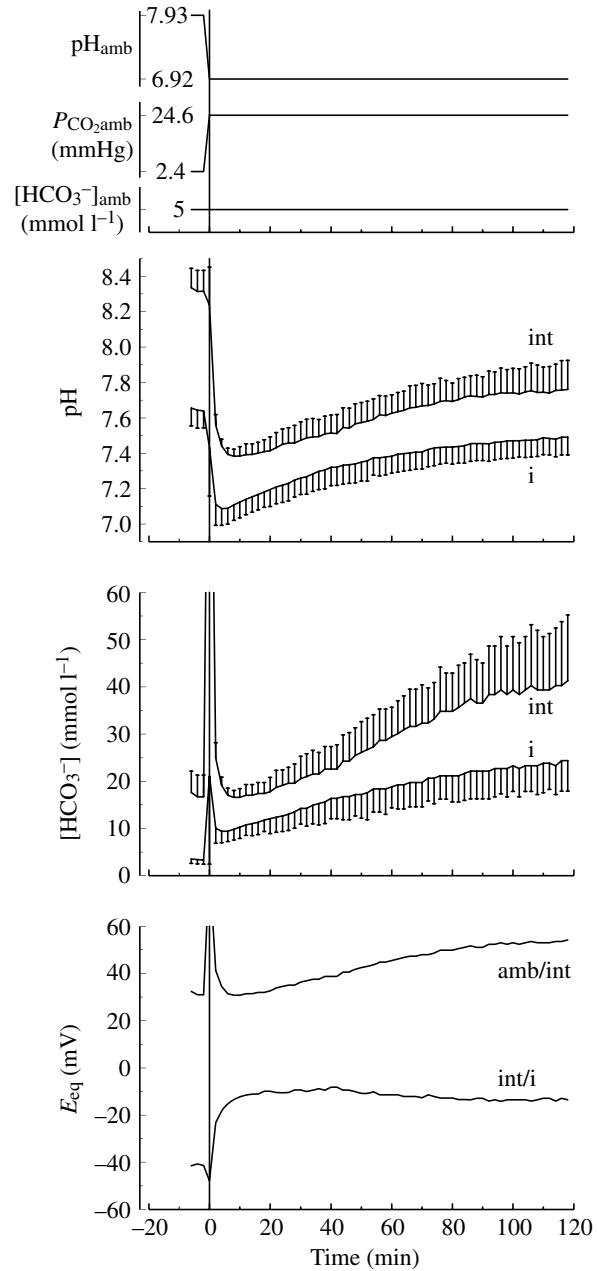


Fig. 5. Hypercapnia in *Danio rerio*. pH, $[HCO_3^-]$ and HCO_3^- equilibrium potentials (E_{eq} ; according to the Nernst equation) of fluid compartments of *Danio* embryos in response to 10-fold changes in P_{CO_2} from 2.4 to 24.6 mmHg. Indices denote: amb, ambient; int, interstitial; i, intracellular. Each point represents the mean of 14 (i) or 5 (int) measurements \pm S.D.

avoids a number of disadvantages compared with other methods. Widely used distribution techniques applying endogenous (e.g. $\text{CO}_2/\text{HCO}_3^-$, ammonia) or exogenous [e.g. DMO (dimethylxazolidinedione), nicotine] indicator substances are generally hampered by their destructive sampling of studied tissues, not allowing direct time series. Further limitations exist in poor spatial and time resolution as well as in the misestimate of average pH according to

subcellular distribution gradients (cf. Heisler, 1989; Hinke and Menard, 1978). Although the principle of microelectrodes avoids these limitations, electrodes small enough not to disturb cellular homeostasis are subject to physical destruction or loss of location with even minute movements of subject or instrumentation, limiting this technique to single culture cells or completely immobilized small tissue samples. With this background, determination of pH by optical analysis of

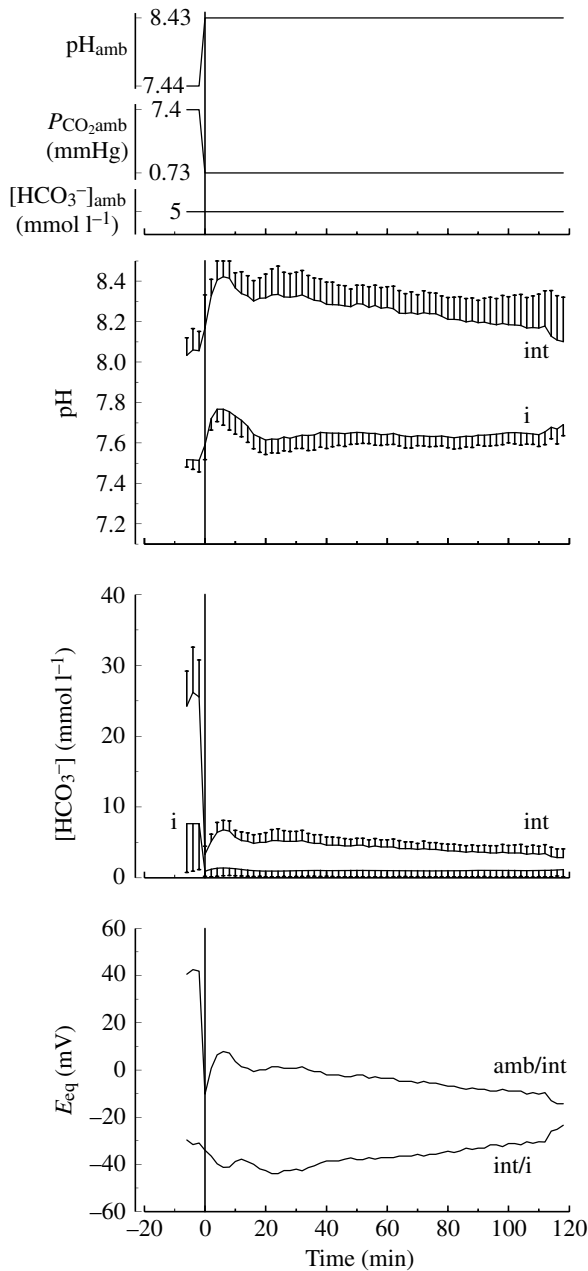


Fig. 6. Post-hypercapnia in *Danio rerio*. pH, $[\text{HCO}_3^-]$ and HCO_3^- equilibrium potentials (E_{eq} ; according to the Nernst equation) of fluid compartments of *Danio* embryos in response to 10-fold changes in P_{CO_2} from 7.4 to 0.73 mmHg. Indices denote: amb, ambient; int, interstitial; i, intracellular. Each point represents the mean of 7 (i) or 6 (int) measurements \pm s.d.

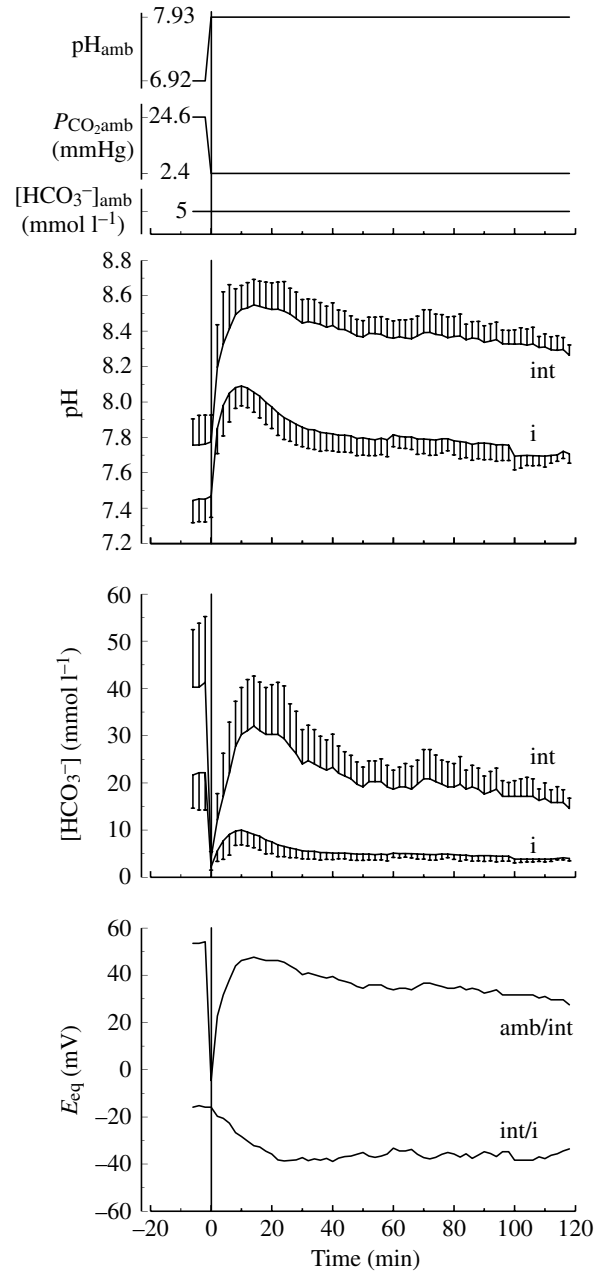


Fig. 7. Post-hypercapnia in *Danio rerio*. pH, $[\text{HCO}_3^-]$ and HCO_3^- equilibrium potentials (E_{eq} ; according to the Nernst equation) of fluid compartments of *Danio* embryos in response to 10-fold changes in P_{CO_2} from 24.6 to 2.4 mmHg. Indices denote: amb, ambient; int, interstitial; i, intracellular. Each point represents the mean of 14 (i) or 5 (int) measurements \pm s.d.

indicator ionization is apparently a most advantageous technique. Accurate and repeatable analysis by optical techniques, however, requires a number of prerequisites evidently not so easily provided.

Methodological resolution as a function of optical stability

One of the most critical factors for optical ion analysis is constancy of used instrumentation. However, fluorescence intensities and, in particular, laser excitation intensities measured in the course of the present study under highly controlled conditions (advanced optical bench, decoupled from any vibrational disturbance and floating on a gas-suspended large mass base) were extremely unstable, an amazing fact in face of the wide use and the popularity of confocal laser scanning microfluorometry for quantitative investigations. Comparative tests on five confocal laser scanning microscopes (four different models of two brands) resulted in similar instabilities of signal intensities (A. Möllich and N. Heisler, unpublished), suggesting that the extensive light processing and the stabilization of laser intensities in confocal microscopes are still grave common problems. Most astonishingly, no report concerning this evidently major methodological limitation was found in the literature.

The obvious deficiency of instrumentation and the resulting error of up to 80% becomes particularly apparent during dual excitation but is partially corrected for by carrying along a fluorescent uranium glass standard with each determination, thus reducing the extreme long term instability to approximately $\pm 6\%$. The residual variability is related to equivalent short-term laser intensity variation, picked up due to the time delay between four required emission measurements (for each of two excitations at two different wavelengths for sample and standard). Thus, with present instrumentation, single-excitation/single-emission as well as dual-excitation/single-emission dyes are deemed unsuitable to provide the pH resolution required for scientific research.

Dual-emission measurement upon single excitation will cancel out any instabilities related to the excitation path, including laser and further optical equipment like AOTF, lenses, splitters, filters, etc. Accordingly, ratios obtained in the course of the present study were improved considerably with the dual-emission dye SNARF-1 as compared with dual-excitation measurements. To our surprise, however, even simultaneous recording with two emission detectors, eliminating the influence of any laser variability, did not reduce the obtained ratio noise to the low levels expected from passive optical components on an advanced, gas-floating optical bench. The residual noise is probably attributable to mechanical instabilities between optical components of the emission light paths. Unfortunately, these variabilities reduced resolution of the method far below the possible limit. The observed maximal variation of the emission ratio ($\pm 2\%$) is equivalent to ± 0.020 pH units as compared with the theoretical resolution of 0.004 units, the limit by 8-bit digitization.

Although the available instrumentation provides relatively coarse restrictions as compared with precision electrode

analyses (<0.001 ; Heisler, 1978), the present study could not have been conducted with anything other than optical techniques. Repeated sampling in a developing organism is clearly impossible with indicator distribution techniques. Microelectrodes, used to calibrate the optical techniques in absolute terms, could not be kept in dividing cells of a growing embryo for more than 30–40 min, definitely not for the 8 h of a full experimental run. Also, microelectrodes could not be produced that were stable enough to be maintained for measurement at a site in a high-protein environment for such a long time without recalibration.

Calibration of optical methods

One major problem in applying microfluorometric techniques is calibration of the indicator emission signal. The interaction of dyes with numerous biological modulators at the site of measurement renders *in situ* calibration with ionophores like nigericin an advantageous procedure, which is actually widely used in isolated culture cells. In excised tissues and multicellular organisms, however, nigericin application is hampered by many factors. In embryos, integrity and viability is impaired by nigericin, and application often results in complete disintegration of the organism, related to loss of adequate membrane potential, pH_i or other cell functions. Further problems are provided by the necessity to achieve a defined nigericin concentration at the site of calibration, in order to equalize pH and ionic concentrations at the studied interface. In intact organisms or tissue chunks, diffusion of nigericin is inhibited by long diffusion paths or interlaced epithelia. Applying the technique to embryos, circumventing the precursors of epithelial cells by direct injection of nigericin is most difficult, if not impossible. Also, the imperatively required measurement of 'extracellular' pH is hard to conduct before an adequately large defined extracellular volume has developed during ontogeny. A major drawback of nigericin is contamination of experimental equipment, hard to get rid of and largely affecting consecutive experiments (Richmond and Vaughan-Jones, 1993).

The accuracy of nigericin calibration, i.e. equalization of ionic composition between two fluid compartments, is not comparable with other techniques applied in acid–base physiology (cf. Heisler, 1989). Even in single culture cells, pH_i differences of 0.15 (Nett and Deitmer, 1996) or 0.06–0.11 (Chaillet and Boron, 1985) have been reported in comparison with microelectrodes, differences larger than the maximal error after *in vitro* calibration with mock intracellular fluid (0.07; for calibration with 10% BSA + 150 mmol l⁻¹ KCl; see above and Fig. 3). Smaller differences observed in comparison with indicator distribution techniques (0.03, Pärt and Wood, 1996; 0.05, Thomas et al., 1979) are biased by the inherent alkaline shift error of such techniques (cf. Heisler, 1989; Hinke and Menard, 1978). For multicellular/multilayer organisms or preparations, literature data of direct comparison of nigericin with microelectrodes are not available.

As a consequence, for this study the optical system was calibrated *in vitro* with standardized 100 mmol l⁻¹ phosphate

buffers, and the data obtained from *in vivo* measurements were adjusted by mathematical post-processing based on *in vivo* simultaneous, at-site comparison with microelectrodes. After having established the correlation between the two techniques, this type of calibration is much easier, while providing much higher accuracy than any other approach. Since specific characteristics of the optical light paths of used instrumentation are accounted for by the procedure, the obtained relationships (cf. Eqns 2 and 3) can be extrapolated to other systems similar in their intracellular composition. This essentially applies to vertebrate cells and interstitial fluid, respectively, with similar [protein], $[K^+]$, ionic strength, etc., and SNARF-1 measurements with single excitation (488 nm) and dual emission (570–590 nm and >630 nm).

This approach of directly correlating microelectrode readout with optical data carries the advantage of eliminating any differences between the two techniques. Microelectrodes are considered as a most reliable basic reference, in spite of the fact that electrodes may certainly be subject to spurious bridge potentials, cross sensitivities and effects of media composition (e.g. Ammann et al., 1981; Siggaard-Andersen, 1961). The microelectrode assemblies utilized in the present study were tested thoroughly before use but did not indicate any cross-sensitivities such as to variable CO_2 and $[HCO_3^-]$, high $[K^+]$, high BSA concentration, ionic strength and other factors in the physiological pH range. The observed typical non-linear response and media sensitivity of individual electrodes below pH 6 (Ammann et al., 1981) is irrelevant on the basis of the utilized pH range between 7.0 and 8.2. Referencing the used microelectrodes with NBS (National Bureau of Standards) phosphate buffer solutions with an accuracy of ± 0.005 , the directly correlated optical techniques are considered to provide comparable accuracy. The repeatability of the approach was determined from time series of standard measurements to be ± 0.020 (maximal deviation), with this limitation compared with the theoretical resolution by 8-bit digitization of 0.004 mainly attributable to instabilities of optical apparatus.

Acid–base regulation in embryonic zebrafish

Intracellular pH is one of the key parameters for modulation of many cellular functions, including general cellular metabolism *via* enzyme activities, cell aggregation and cytoskeleton formation (for a review, see Busa and Nuccitelli, 1984; Putnam and Roos, 1997). Thus, development of pH regulation represents an important step of ontogeny. Under control steady-state conditions, pH_i is apparently adjusted to a fairly constant setpoint value (7.55 ± 0.13). The transmembrane pH difference between intracellular space of not yet differentiated embryonic cells and the interstitial space (8.08 ± 0.25) of about 0.5 units at 25°C is comparable with the conditions in muscle tissues of adult fish (~ 0.6 ; Heisler, 1986b, 1993). However, the absolute level of pH_i is higher by 0.3–0.4 than in adult fish (general range in muscle, with few exceptions, 7.05–7.30 at 25°C; Heisler, 1986b), leading to more than twice as high embryonic $[HCO_3^-]$ for the same P_{CO_2} . Thus, for a given effect in pH, twice as much bicarbonate has

to be transferred across membranes and ‘epithelia’. On the other hand, a higher level of bicarbonate provides a higher bicarbonate buffer value (Heisler, 1986a, 1989), which may become useful under conditions of transient anoxia with production of organic acids dissociating H^+ ions.

Regulation of pH is generally based on passive distribution of HCO_3^- on the basis of the membrane potential, eventually supplemented by active transfer processes for final adjustment deviating from passive distribution (cf. Heisler, 1986a). At the observed levels, adjustment of embryonic pH_i is impossible on the basis of passive mechanisms alone. The equilibrium potential for HCO_3^- transmembrane distribution in steady-state embryos, calculated from the Nernstian relationship, varies between -20 and -40 mV (Figs 4, 5). This is significantly different from typical membrane potentials of fish embryonic cells (-60 to -70 mV, Bregestovski et al., 1992; -71 mV, Buss and Drapeau, 2000). These relationships strongly suggest an energy-demanding process for active distribution of bicarbonate.

While active transport is definitely involved in pH_i adjustment, the regulatory capacity of the process is difficult to evaluate. During steady state, the required activity depends largely on the rate of HCO_3^- leakage (or of other acid–base relevant ions) across the membrane. Thus, with tight compartmental interfaces, the active process may suffice regulatory demands in spite of an extremely low capacity. This also holds for the apparent independence of cellular pH during metabolic (non-respiratory) challenges of ambient pH found in the present study, results confirmed in a variety of fish embryos (e.g. Johansson et al., 1973, 1977).

Direct challenge of cellular and interstitial pH regulation by changes of ambient P_{CO_2} is readily transmitted to the intracellular fluid compartments, independent of ionic permeation characteristics of membranes. The maximal deflection of pH after changes in P_{CO_2} may be taken as an expression of available non-bicarbonate buffering in the respective compartment, but only with caution ($\beta_{NB,app}$; cf. Heisler, 1986a). Values obtained in cells at this stage (10 – 25 meq. $pH^{-1} l^{-1}$ cell H_2O) are lower than chemical nonbicarbonate buffer values of adult fish specimens (33 – 49 meq. $pH^{-1} l^{-1}$ cell H_2O ; cf. Heisler, 1986a). Deviations between embryos and adults are probably attributable to exchange of HCO_3^- equivalents with the environment as an expression of not yet adjusted thresholds at membrane and ‘epithelial’ levels, as was found in *Scyliorhinus* (Heisler et al., 1976). Interstitial $\beta_{NB,app}$ values at maximal pH deflection are generally much higher than the expected rather low chemical buffering ability of this fluid space (cf. Heisler, 1986a) and are definitely an expression of bicarbonate originating from other fluid compartments such as cells, yolk and/or surrounding embryonic fluid. During the following ~ 2 h, large changes in bicarbonate in both intracellular as well as interstitial spaces indicate transfer of acid–base relevant ions for compensation of these two fluid compartments from the ambient fluid as the only available significant source (Heisler, 1984). The extremely small interstitial space (estimated to be 5–8% of the organism at this ontogenetic state) functions as a transit fluid

volume rather than providing bicarbonate for the compensation of the intracellular space. As a result of bicarbonate accumulation, the $\beta_{\text{NB,app}}$ after 2 h is largely elevated in both studied compartments.

Net transfer of bicarbonate from interstitial to intracellular space is definitely an active process for the two series of P_{CO_2} elevation (0.73 to 7.4 and 2.4 to 24.6 mmHg). The equilibrium potential of bicarbonate shifts during high P_{CO_2} from the control range of -30 to -40 mV closer to zero, thus even enhancing the electrochemical force against compensatory cellular influx of HCO_3^- . Accordingly, the kinetics for bicarbonate accumulation during hypercapnia are slower than the release of bicarbonate equivalents from the cells after return to low-level P_{CO_2} s (cf. Figs 4 and 5 vs Figs 6 and 7). In these post-hypercapnia series, the equilibrium potential returns towards the -30 to -40 mV steady-state range, which still provides considerable electrochemical force for compensatory efflux of bicarbonate from the cells. It remains questionable, however, whether the high rate of bicarbonate-equivalent efflux can take place on the basis of passive diffusion alone. More likely, the efflux is supplemented by an active transfer enhancing the kinetics of pH normalization. The finally attained steady-state distribution is definitely maintained by active processes anyway (see above).

Also, comparison of bicarbonate distribution potentials between interstitium and ambient fluid with actual data yields evidence as to the nature of involved transfer mechanisms. Potentials in adult freshwater fish are found in the range of slightly negative to slightly positive values (-5 to $+10$ mV, inside to outside), depending upon a variety of factors, such as $[\text{Na}^+]$, $[\text{Cl}^-]$ and, in particular, $[\text{Ca}^{2+}]$ (Eddy, 1975; Kerstetter et al., 1970; Kerstetter and Kirschner, 1972). The HCO_3^- equilibrium potentials at low-level P_{CO_2} calculated for the present study are close to this range. During changes in P_{CO_2} , however, the equilibrium potential is largely shifted to attain values between -20 and $+55$ mV. Differential diffusion of Na^+ and Cl^- , responsible for the interstitial/ambient potential, is largely affected by the presence of Ca^{2+} but is relatively insensitive to changes in P_{CO_2} and $[\text{HCO}_3^-]$. The transepithelial potential in goldfish is shifted by only 5 mV upon 100-fold changes of the bicarbonate distribution ratio (Eddy, 1975). These interrelationships strongly suggest that HCO_3^- is distributed between embryonic interstitium and ambient fluid by active processes located in the outer cell layer (structurally not yet 'epithelium') of the embryo.

Quantification of acid-base relevant ion fluxes between cells, interstitium and ambient water is difficult on the basis of the present approach. The observed kinetics of changes in intracellular $[\text{HCO}_3^-]$ and pH, however, suggest much higher transfer rates than typically found in adult fish exposed to hypercapnia (Heisler, 1982, 1984, 1986b, 1993). This may, at least partially, be related to relatively high $[\text{Na}^+]$, $[\text{HCO}_3^-]$ and $[\text{Ca}^{2+}]$ in the ambient fluid (embryonic medium; in mmol l^{-1} : $[\text{Na}^+]$ 19, $[\text{Ca}^{2+}]$ 1.3, $[\text{HCO}_3^-]$ 5), supporting acid-base relevant ion exchange (cf. Heisler, 1999), but transfer of bicarbonate equivalents to the intracellular compartment will

also be advanced by the small capacity and accordingly quick compensation of the interstitial space, supporting cellular adjustments.

Evidently, the stress of hypercapnia is suitable to activate membrane ion transfer processes in embryos, but, although the observed rate is high as compared with adult fish, it may not represent the full capacity of mechanisms. As is well known from similar experiments in adult fish, the rate of ion transfer processes largely depends on the nature of stress (e.g. temperature changes vs severe lactacidosis; Heisler, 1978, 2004; Holeton et al., 1983), suggesting graded reaction to different stimuli.

Abrupt changes of intracellular pH are initiated in oocytes by sperm fusion. Data in zebrafish are unavailable, but a few literature reports indicate pH_i alkaline shifts of 0.2–0.3 in *Xenopus* embryos (e.g. Webb and Nuccitelli, 1981), to attain a much higher range of 7.6–7.7 than found in adult specimens (7.0–7.1; e.g. Boutilier et al., 1987). Even slightly larger shifts of 0.3–0.4 units are found in sea urchin and clam oocytes (e.g. Johnson and Epel, 1981; Dubé and Eckberg, 1997). The alkalization upon sperm fusion is considered to follow activation of a Na^+/H^+ exchanger in these species (Dubé and Eckberg, 1997; Gusev, 2001). During further embryonic development, the Na^+/H^+ exchanger, as well as HCO_3^- related transporters, is known to be modulated by a variety of growth factors (Moolenaar, 1986; Boron and Boulpaep, 1989).

Although pH_i is a proven factor of large importance in energy metabolism, in embryos the effect of shifts in pH on further development is diverse, the range spanning from hardly any effect in *Xenopus* (e.g. Stith and Maller, 1985), an optimized protein synthesis at elevated pH in sea urchins (Rees et al., 1995) to a pronounced correlation of development with pH_i in echiuroids (Gould and Stephano, 1993). In zebrafish, general ontogeny was not affected at all by a wide range of hypercapnia and the associated changes in pH. Evidently, numerous factors are involved in this complex pattern of regulation, and their interaction has to remain the subject of further experimentation.

Conclusions

(1) Microfluorometric techniques facilitate continuous recordings of pH_i and pH_{int} with high spatial and time resolution for more than 8 h in developing fish embryos.

(2) High-accuracy calibration in complex organisms can be performed by *in vitro* inorganic buffer calibration, with mathematical post-processing according to *in vivo* simultaneous, at-site comparison of optical techniques with microelectrodes accounting for biological dye modulation.

(3) The theoretical accuracy inherent in dual-wavelength microfluorometric analysis can only partially be exploited with commercially available instrumentation because of extensive instability.

(4) *Danio rerio* embryos are capable of tightly adjusting and maintaining cellular and interstitial pH from early stages during long phases of ontogeny (stage 1k-cells to end of epiboly).

(5) Non-respiratory changes of ambient pH do not affect cellular pH, indicating high effective resistance of cellular membranes to uncontrolled diffusion of acid–base relevant ions.

(6) Active ion transfer mechanisms in embryos provide higher capacity to compensate extensive direct stress of cellular pH regulation than found in comparable adult organisms.

We thank Dr Juha Voipio for his invaluable support in constructing pH microelectrodes.

References

- Ammann, D., Lanter, F., Steiner, R. A., Schulthess, P., Shijo, Y. and Simon, W.** (1981). Neutral carrier based hydrogen ion selective microelectrode for extra and intracellular studies. *Anal. Chem.* **53**, 14, 2267–2269.
- Boron, W. F. and Boulpaep, E. L.** (1989). The electrogenic $\text{Na}^+/\text{HCO}_3^-$ cotransporter. *Kidney Int.* **36**, 392–402.
- Boutilier, R. G., Glass, M. L. and Heisler, N.** (1987). Blood gases, and extracellular/intracellular acid–base status as a function of temperature in the anuran amphibians *Xenopus laevis* and *Bufo marinus*. *J. Exp. Biol.* **130**, 13–25.
- Bregestovski, P., Medina, I. and Goyda, E.** (1992). Regulation of potassium conductance in the cellular membrane at early embryogenesis. *J. Physiol.* **86**, 109–115.
- Bright, G. R., Whitaker, J. E., Haugland, R. P. and Taylor, D. L.** (1989). Heterogeneity of the changes in cytoplasmic pH upon serum stimulation of quiescent fibroblasts. *J. Cell Physiol.* **141**, 410–419.
- Busa, W. B. and Nuccitelli, R.** (1984). Metabolic regulation via intracellular pH. *Am. J. Physiol.* **246**, R409–R438.
- Buss, R. R. and Drapeau, P.** (2000). Physiological properties of zebra fish embryonic red and white muscle fibres during early development. *J. Neurophysiol.* **84**, 1545–1557.
- Chaillet, J. R. and Boron, W. F.** (1985). Intracellular calibration of a pH-sensitive dye in isolated, perfused salamander proximal tubules. *J. Gen. Physiol.* **86**, 765–794.
- Claiborne, J. B.** (1998). Acid–base regulation. In *The Physiology of Fishes*, 2nd edition (ed. D. H. Evans), pp. 177–198. Boca Raton, New York: CRC Press.
- Dubé, F. and Eckberg, W. R.** (1997). Intracellular pH increase driven by an Na^+/H^+ exchanger upon activation of surf clam oocytes. *Dev. Biol.* **190**, 41–54.
- Duis, K. and Oberemm, A.** (2000). Survival and sublethal responses of early life stages of pike exposed to low pH in artificial postmining lake water. *J. Fish Biol.* **57**, 597–613.
- Eddy, F. B.** (1975). The effect of calcium on gill potentials and on sodium and chloride fluxes in the goldfish, *Carassius auratus*. *J. Comp. Physiol.* **96**, 131–142.
- Epel, D.** (1997). Activation of sperm and egg during fertilisation. In *Handbook of Physiology*, vol. **14**, *Cell Physiology* (ed. J. F. Hoffman and J. D. Jamieson), pp. 859–884. New York, Oxford: Oxford University Press.
- Gould, M. and Stephano, J. L.** (1993). Nuclear and cytoplasmic pH increase at fertilisation in *Urechis caupo*. *Dev. Biol.* **159**, 608–617.
- Gusev, G. P.** (2001). Na^+/H^+ exchanger in tissues of lower vertebrates. *J. Evol. Biochem. Physiol.* **37**, 595–603.
- Heisler, N.** (1978). Bicarbonate exchange between body compartments after changes of temperature in the larger spotted dogfish (*Scyliorhinus stellaris*). *Respir. Physiol.* **33**, 145–160.
- Heisler, N.** (1982). Transepithelial ion transfer processes as mechanisms for fish acid–base regulation in hypercapnia and lactacidosis. *Can. J. Zool.* **60**, 1108–1122.
- Heisler, N.** (1984). Acid–base regulation in fishes. In *Fish Physiology*, vol. Xa (ed. W. S. Hoar and D. J. Randall), pp. 315–401. Orlando: Academic Press.
- Heisler, N.** (1986a). Buffering and transmembrane ion transfer processes. In *Acid–Base Regulation in Animals* (ed. N. Heisler), pp. 3–47. Amsterdam: Elsevier.
- Heisler, N.** (1986b). Acid–base regulation in fishes. In *Acid–Base Regulation in Animals* (ed. N. Heisler), pp. 309–356. Amsterdam: Elsevier.
- Heisler, N.** (1986c). Comparative aspects of acid–base regulation. In *Acid–Base Regulation in Animals* (ed. N. Heisler), pp. 397–450. Amsterdam: Elsevier.
- Heisler, N.** (1989). Parameters and methods in acid–base physiology. In *Techniques in Comparative Respiratory Physiology – An Experimental Approach*, SEB Seminar Series (ed. C. R. Bridges and P. J. Butler), pp. 305–332. Cambridge, UK: Cambridge University Press.
- Heisler, N.** (1993). Acid–base regulation. In *The Physiology of Fishes*, 1st edition (ed. D. H. Evans), pp. 343–378. Boca Raton, New York: CRC Press.
- Heisler, N.** (1999). Limiting factors for acid–base regulation in fish: branchial transfer capacity vs. diffusive loss of acid–base relevant ions. In *Regulation of Tissue pH in Plants and Animals*, SEB Seminar Series (ed. S. Egginton, E. W. Taylor and J. A. Raven), pp. 125–154. Cambridge, UK: Cambridge University Press.
- Heisler, N.** (2004). Buffering and H^+ ion dynamics in muscle tissues. *Resp. Physiol. Neurobiol.* **144**, 161–172.
- Heisler, N., Weitz, H. and Weitz, A. M.** (1976). Hypercapnia and resultant bicarbonate transfer processes in an elasmobranch fish (*Scyliorhinus stellaris*). *Bull. Eur. Physiopath. Respir.* **12**, 77–85.
- Hinke, J. A. M. and Menard, M. R.** (1978). Evaluation of the DMO method for measuring intracellular pH. *Resp. Physiol.* **33**, 31–40.
- Holeton, G. F., Neumann, P. and Heisler, N.** (1983). Branchial ion exchange and acid–base regulation after strenuous exercise in rainbow trout (*Salmo gairdneri*). *Resp. Physiol.* **51**, 303–318.
- Ingersoll, C. G., Mount, D. R., Gulley, D. D., La Point, T. W. and Bergman, H. L.** (1990). Effects of pH, aluminium, and calcium on survival and growth of eggs and fry of brook trout (*Salvelinus fontinalis*). *Can. J. Fish Aquat. Sci.* **47**, 1580–1592.
- Johansson, N., Kihlström, J. E. and Wahlberg, A.** (1973). Low pH values shown to affect developing fish eggs (*Brachydanio rerio* Ham. Buch.) *AMBIO* **2**, 42–43.
- Johansson, N., Runn, P. and Milbrink, G.** (1977). Early development of three salmonid species in acidified water. *Zoon* **5**, 127–132.
- Johnson, C. H. and Epel, D.** (1981). Intracellular pH of sea urchin eggs measured by the dimethylxazolinedione (DMO) method. *J. Cell Biol.* **89**, 284–291.
- Kerstetter, F. H., Kirschner, L. B. and Rafuse, D. D.** (1970). On the mechanism of sodium ion transport by the irrigated gills of rainbow trout (*Salmo gairdneri*). *J. Gen. Physiol.* **56**, 342–359.
- Kerstetter, F. H. and Kirschner, L. B.** (1972). Active chloride transport by the gills of rainbow trout (*Salmo gairdneri*). *J. Exp. Biol.* **56**, 263–272.
- Kimmel, C. B., Ballard, W. W., Kimmel, S. R., Ullmann, B. and Schilling, T. F.** (1995). Stages of embryonic development of the zebrafish. *Dev. Dyn.* **203**, 253–310.
- Lacroix, G. L. and Townsend, D. R.** (1987). Responses of juvenile atlantic salmon (*Salmo salar*) to episodic increases in acidity of Nova Scotia rivers. *Can. J. Fish. Aquat. Sci.* **44**, 1475–1484.
- Moolenaar, W. H.** (1986). Effects of growth factors on intracellular pH regulation. *Annu. Rev. Physiol.* **48**, 363–376.
- Nett, W. and Deitmer, J. W.** (1996). Simultaneous measurements of intracellular pH in the leech giant glial cell using 2,7-bis-(2-Carboxyethyl)-5,6-carboxyfluorescein and ion-sensitive microelectrodes. *Biophys. J.* **71**, 394–402.
- Pärt, P. and Wood, C. M.** (1996). Na^+/H^+ exchange in cultured epithelial cells from fish gills. *J. Comp. Physiol. B* **166**, 37–45.
- Potts, W. T. W. and McWilliams, P. G.** (1989). The effect of hydrogen and aluminium ions on fish gills. In *Acid Toxicity and Aquatic Animals* (ed. R. Morris, E. W. Taylor, D. J. A. Brown and J. A. Brown), pp. 201–220. Cambridge, UK: Cambridge University Press.
- Pressman, B. C.** (1976). Biological applications of ionophores. *Annu. Rev. Biochem.* **45**, 501–530.
- Putnam, R. W. and Roos, A.** (1997). Intracellular pH. In *Handbook of Physiology*, vol. **14**, *Cell Physiology* (ed. J. F. Hoffman and J. D. Jamieson), pp. 389–440. New York, Oxford: Oxford University Press.
- Rees, B. B., Patton, C., Grainger, J. L. and Epel, D.** (1995). Protein synthesis increases after fertilization of sea urchin eggs in the absence of an increase in intracellular pH. *Dev. Biol.* **169**, 683–698.
- Richmond, P. and Vaughan-Jones, R. D.** (1993). K^+/H^+ exchange in isolated carotid body type-1 cells of the neonatal rat is caused by nigericin contamination. *J. Physiol.* **467**, 277.
- Siggaard-Andersen, O.** (1961). Factors effecting the liquid-junction potential in electrometric blood pH measurement. *Scand. J. Clin. Lab. Invest.* **13**, 205–211.

- Sprague, J., Doerry, E., Douglas, S. and Westerfield, M.** (2001). The Zebrafish Information Network (ZFIN): a resource for genetic, genomic and developmental research. *Nucleic Acids Res.* **29**, 87-90.
- Stith, B. J. and Maller, J. L.** (1985). Increased intracellular pH is not necessary for ribosomal protein S6 phosphorylation, increased protein synthesis, or germinal vesicle breakdown in *Xenopus* oocytes. *Dev. Biol.* **107**, 460-469.
- Thomas, J. A., Buchsbaum, R. N., Zimniak, A. and Racker, E.** (1979). Intracellular pH measurement in Ehrlich ascites tumor cells utilizing spectroscopic probes generated in situ. *Biochemistry* **18**, 2210-2218.
- Voipio, J., Pasternack, M. and MacLeod, K.** (1994). Insensitive microelectrodes. In *Microelectrode Techniques. The Plymouth Workshop Handbook*, 2nd edition (ed. D. Ogden), pp. 275-316. Cambridge, UK: The Company of Biologists Ltd.
- Webb, D. J. and Nuccitelli, R.** (1981). Direct measurement of intracellular pH changes in *Xenopus* eggs at fertilisation and cleavage. *J. Cell Biol.* **91**, 562-567.
- Westerfield, M.** (1995). *The Zebrafish Book. A Guide For The Laboratory Use of the Zebrafish (Danio rerio)*, 3rd edition. Eugene: University of Oregon Press.
- Whitaker, J. E., Haugland, R. P. and Prendergast, F. G.** (1991). Spectral and photophysical studies of benzo[c]xanthene dyes: dual emission pH sensors. *Anal. Biochem.* **194**, 330-344.
- Wood, C. M., McDonald, D. G., Ingersoll, C. G., Mount, D. R., Johannsson, O. E., Landsberger, S. and Bergman, H. L.** (1990a). Effects of water acidity, calcium, and aluminium on whole body ions of brook trout (*Salvelinus fontinalis*) continuously exposed from fertilisation to swim-up: a study by instrumental neutron activation analysis. *Can. J. Fish Aquat. Sci.* **47**, 1593-1603.
- Wood, C. M., McDonald, D. G., Ingersoll, C. G., Mount, D. R., Johannsson, O. E., Landsberger, S. and Bergman, H. L.** (1990b). Whole body ions of brook trout (*Salvelinus fontinalis*) alevins: responses of yolk-sac and swim-up stages to water acidity, calcium, and aluminium, and recovery effects. *Can. J. Fish Aquat. Sci.* **47**, 1604-1615.